

This is the accepted manuscript made available via CHORUS. The article has been published as:

## Enhancing the Intense Field Control of Molecular Fragmentation

Fatima Anis and B. D. Esry

Phys. Rev. Lett. **109**, 133001 — Published 25 September 2012

DOI: [10.1103/PhysRevLett.109.133001](https://doi.org/10.1103/PhysRevLett.109.133001)

# Enhancing the intense field control of molecular fragmentation

Fatima Anis and B. D. Esry

*J.R. Macdonald Laboratory, Kansas State University, Manhattan, Kansas 66506*

We describe a pump-probe scheme with which the spatial asymmetry of dissociating molecular fragments — as controlled by the carrier-envelope phase of an intense few-cycle laser pulse — can be enhanced by an order of magnitude or more. We illustrate the scheme using extensive, full-dimensional calculations for dissociation of  $\text{H}_2^+$  and include the averaging necessary for comparison with experiment.

In recent years, considerable experimental effort has been invested in developing the ability to control chemical reactions with intense, few-cycle laser pulses [1–4]. The canonical reaction chosen has been molecular dissociation, and a common measure of the degree of its coherent control is the spatial asymmetry of fragments relative to a linearly polarized laser field. Quantum mechanically, this asymmetry arises from the interference of pathways that lead to even and odd parity states [5–7]. In strong fields, these pathways can involve many photons, and the relative phase between the pathways — and thus the outcome — can be controlled by varying the laser parameters such as the carrier envelope phase (CEP) (see, for example, Refs. [1–4, 6–15]) or the relative phase between different colors (see, for example, Refs. [16–27]). In this Letter, we will focus on control via the CEP.

In the dipole approximation, the CEP  $\varphi$  for a Gaussian laser pulse  $\mathcal{E}(t)$  is defined from [28]

$$\mathcal{E}(t) = \mathcal{E}_0 e^{-t^2/\tau^2} \cos(\omega t + \varphi). \quad (1)$$

Generally, the largest CEP-dependent asymmetries have been observed for ionized electrons [1]. The asymmetries for the nuclear fragments resulting from dissociation have, unfortunately, been much smaller [3, 9, 10]. These weak effects — combined with the ongoing challenge of producing intense, few-cycle, CEP stabilized pulses — greatly limit experimentalists’ abilities to measure and explore this intriguing means of control. One important recent advance is the ability to measure the CEP of each pulse [29, 30], alleviating the need for CEP stability during the measurements.

We have previously shown [6, 7, 12] that CEP effects can generally and rigorously be understood as resulting from the interference of pathways involving different net numbers of photons with the CEP entering only their relative phase. For instance, CEP-dependent spatial asymmetry in dissociation results primarily from the interference of  $n$ - and  $(n+1)$ -photon pathways that end at the same final energy [7] since dipole selection rules dictate that they will have opposite parity. Moreover, in this case, our formulation predicts that the asymmetry will be a linear combination of  $\sin \varphi$  and  $\cos \varphi$ . In order for  $n$ - and  $(n+1)$ -photon processes to contribute at the same final energy, the bandwidth must be large; and thus the pulse, short. Finally, the largest CEP effects will result

when the  $n$ - and  $(n+1)$ -photon amplitudes are comparable in magnitude, requiring relatively high intensity.

While CEP-dependent asymmetric break up of  $\text{H}_2^+$  was predicted a few years ago [2], successful measurements have not yet been made starting directly from this benchmark system, *e.g.* in an ion beam experiment [31]. Experiments have instead begun with the more complicated  $\text{H}_2$  [3, 4, 10]. With only one electron, the number of control pathways for  $\text{H}_2^+$  is smaller than for  $\text{H}_2$  making the interpretation more straightforward. Moreover, the theory at sub-ionization intensities can be done essentially exactly [32].

The technical challenges of an ion beam experiment [33] are obvious reasons that the  $\text{H}_2^+$  experiments have not yet been done. However, a more fundamental problem — and one shared by many other molecules — lies in the fact that  $\text{H}_2^+$  typically comes in a broad rovibrational distribution in such experiments [33]. Unfortunately, dissociation of  $\text{H}_2^+$  from different initial  $v$  by a linearly polarized laser pulse gives fragments with similar energies. Since the asymmetry varies rather dramatically with  $v$  — from larger asymmetry due to the interference of  $n=2$  and 3 for lower  $v$  to essentially no asymmetry from higher  $v$  with primarily  $n=1$  [7, 34–37], the incoherent averaging over initial  $v$  required for an  $\text{H}_2^+$  beam tends to wash out the overall asymmetry [38]. Moreover, one-photon dissociation of higher  $v$  dominates the total dissociation signal [32], especially after averaging over the intensity distribution of the laser focus [33]. And, since  $n=1$  implies a single nuclear parity, its momentum distribution is symmetric, masking the desired asymmetry.

In this Letter, we present a scheme to greatly enhance CEP effects and demonstrate it for the benchmark system of  $\text{H}_2^+$ . The enhancement is largely achieved by depleting the undesired higher- $v$  states with a long, weak pump pulse. Subsequent dissociation of this prepared system by a few-cycle probe pulse gives a momentum distribution with an order of magnitude enhanced asymmetry compared to that of the initial incoherent Franck-Condon distribution of  $\text{H}_2^+$ . In fact, our scheme gives larger asymmetries — at longer pulse lengths — than have been observed so far in  $\text{H}_2$  experiments [3, 9, 10, 14]. We also propose ways to separate the pump and probe signals. To support our claims, we present theoretical

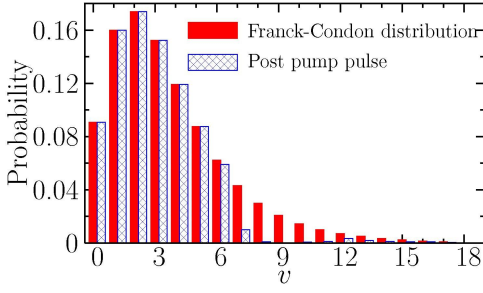


FIG. 1: Vibrational state distribution before and after the 45 fs,  $10^{13}$  W/cm<sup>2</sup> pump pulse.

CEP-dependent  $p+H$  momentum distributions in addition to the up-down asymmetry. Calculating such a differential observable — along with intensity averaging — permits us to quantitatively predict the experimental outcome and to provide deeper physical insight.

To obtain the momentum distribution, it is necessary to account for the nuclear rotation. We thus solve the time-dependent Schrödinger equation in the Born-Oppenheimer representation, including nuclear rotation, nuclear vibration, and electronic excitation, but neglecting ionization as well as the Coriolis and all nonadiabatic couplings. The nuclear rotation is included as an expansion of the wave function over the total orbital angular momentum ( $J$ ) basis (see [32] for details).

To prepare the system, we use a 785 nm, 45 fs long pump pulse with an intensity of  $10^{13}$  W/cm<sup>2</sup>. This relatively long, weak pump pulse depletes the higher  $v$  states, eliminating their spatially symmetric dissociation signal. Figure 1 shows the  $v$ -distribution before and after this pump pulse. In the incoherent Franck-Condon  $v$ -distribution appropriate for an  $H_2^+$  target [33], 9.58% of the population lies in  $v \geq 8$ . Since 90% of this population dissociates in the pump pulse [32],  $v \geq 8$  becomes only 1.36% of the total remaining bound population, ensuring that their contribution to the dissociation signal by any subsequent probe pulse will be negligible. Consequently, we performed probe pulse calculations only including  $v = 0-7$ , after verifying for a representative case that  $v \geq 8$  affected the asymmetry by much less than 1%.

To quantify the enhancement, we compare the results from an initial incoherent Franck-Condon distribution of  $H_2^+$  interacting with *only* the probe pulse (“probe-only”) to the signal from the probe part of our proposed pump-probe scheme (“pump-probe”). We used a 7 fs, 785 nm probe pulse in both cases. In the pump-probe scheme, all calculations were performed at a fixed time delay of 267 fs unless stated otherwise. Since ionization is neglected, we limit the peak intensity to no more than  $1.2 \times 10^{14}$  W/cm<sup>2</sup> [39]. For the peak intensities above  $10^{13}$  W/cm<sup>2</sup> required for intensity averaging, our calcu-

lations included  $p+H(2l)$  manifold in addition to  $1s\sigma_g$  and  $2p\sigma_u$  channels. The total population of the  $p+H(2l)$  states was less than 5% even for the highest intensity. Consequently, we present momentum distributions based on just the  $1s\sigma_g$  and  $2p\sigma_u$  channels.

The fundamental physical observable we focus on is the  $p+H$  relative momentum distribution  $\rho(\mathbf{K})$ , which is the most differential observable in recent experiments involving  $H_2^+$  dissociation [31, 33, 34]. To calculate  $\rho(\mathbf{K})$ , we project the final wave function onto scattering states that behave as  $\exp(i\mathbf{K} \cdot \mathbf{R})\phi_{1sA}$  asymptotically, where  $\mathbf{R}$  points from proton  $A$  to proton  $B$  and  $\phi_{1sA}$  is the hydrogen ground state wave function centered on proton  $A$ . The momentum  $\mathbf{K}$  thus points from  $H$  to  $p$ . This scattering state, with the nuclear spin included, is then symmetrized to account for the identical nuclei [40–42]. Finally, the momentum distribution [or its energy-normalized equivalent  $\rho(E, \hat{K})$  with  $E = K^2/2\mu$ ,  $\mu$  the nuclear reduced mass, and  $\hat{K} = (\theta_K, \varphi_K)$  the direction of  $\mathbf{K}$  with respect to the polarization direction] is

$$\begin{aligned} \rho(\mathbf{K}) &= \frac{1}{\mu\sqrt{2\mu E}} \rho(E, \hat{K}) \\ &= \frac{1}{\mu\sqrt{2\mu E}} \left| \sum_{J \text{ even}} C_{Jg} Y_{JM}(\hat{K}) + \sum_{J \text{ odd}} C_{Ju} Y_{JM}(\hat{K}) \right|^2 \end{aligned} \quad (2)$$

with ( $p = g, u$ )

$$C_{Jp} = C_{Jp}(E) = (-i)^J e^{-i\delta_{Jp}} \langle E J p | F_{Jp}(t_f) \rangle. \quad (3)$$

Here,  $|F_{Jp}(t_f)\rangle$  are the  $1s\sigma_g$  and  $2p\sigma_u$  nuclear radial wave functions at the final time  $t_f$ , while  $|E J p\rangle$  and  $\delta_{Jp}$  are the corresponding energy-normalized scattering states and phase shifts, respectively. Note that the first term of Eq. (2) has even parity while the second has odd parity. It is when both terms contribute at the same energy, as determined by the CEP-dependent  $C_{Jp}(E)$ , that asymmetry will emerge [7].

For simplicity, we have not included a label in Eqs. (2) and (3) to indicate the initial state, but there will be separate  $\rho(\mathbf{K})$  for each initial  $v$ . These  $\rho(\mathbf{K})$  must then be averaged, weighted by the Franck-Condon factors. In the remainder of this Letter, we will exclusively refer to these Franck-Condon-averaged momentum distributions.

Equation (2) shows that although a linear combination of  $1s\sigma_g$  and  $2p\sigma_u$  is necessary to localize the electron as an atomic rather than a molecular state, the spatial asymmetry of  $p+H$  is due to the interference of even and odd nuclear parity states. This distinction is brought into sharp relief when nuclear rotation is included in the calculation since using simply  $1s\sigma_g \pm 2p\sigma_u$  nuclear wave function — as is done in calculations without rotation — would produce two distinct  $p+H$  momentum distributions, where clearly only one can be measured. It is the symmetrization requirement that dictates the proper coherent combination to use. This issue is not new, however, and always arises for identical particle scattering

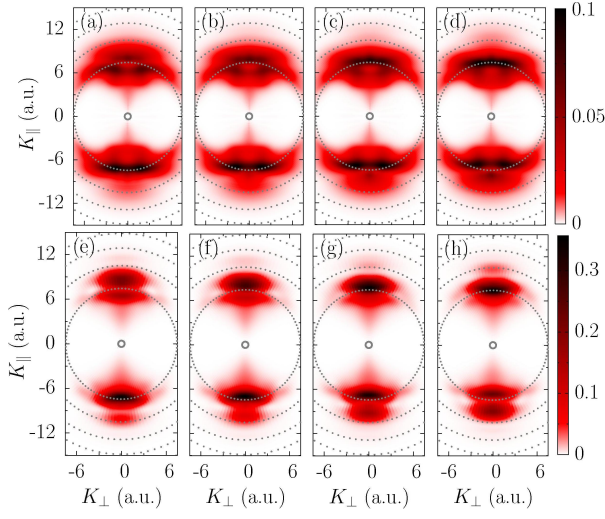


FIG. 2: Franck-Condon-averaged  $K^2 \rho(\mathbf{K})$  (integrated over  $\varphi_K$ ) for probe-only [ $\rho(\mathbf{K})$  is reflected to  $-K_\perp$  for clarity] for (a)  $\varphi = 0$ , (b)  $\varphi = \pi/4$ , (c)  $\varphi = \pi/2$ , and (d)  $\varphi = 3\pi/4$  (Gray dotted lines mark  $K = 7.5, 10, 12.5$ , and  $15$  a.u.). (e)–(h) are same as (a)–(d) but for pump-probe. All cases used a 7 fs,  $10^{14}$  W/cm $^2$  probe pulse.

where it is known that the primary differences occur for  $\theta_K \approx \pi/2$ . Since intense-field dissociation of  $\text{H}_2^+$  produces very few fragments at this  $\theta_K$ , the consequences of analyzing incorrectly are less pronounced. For more complicated systems, however, this need no longer be true.

The Franck-Condon-averaged momentum distributions for several CEPs are shown in Figs. 2(a)–(d) for the probe-only case and in Figs. 2(e)–(h) for the pump-probe case. The momentum distributions in all cases exhibit preferential alignment along the laser polarization. Moreover, since the energy distributions

$$\rho(E) = \int \rho(E, \hat{K}) d\hat{K} \quad (4)$$

for the  $1s\sigma_g$  and  $2p\sigma_u$  channels of individual vibrational states overlap roughly in the range 0.5–1.5 eV, we expect spatial asymmetries to appear roughly for  $6 \leq K \leq 10$  a.u. The results shown in Fig. 2 for both experimental scenarios are consistent with this expectation. The momentum distribution for  $\varphi = \varphi + \pi$  is the mirror image of the momentum distribution for  $\varphi$ , as guaranteed by the fact that  $\cos(\omega t + \pi) = -\cos \omega t$  in Eq. (1).

While the two experimental scenarios clearly show qualitative differences, the strikingly different distributions make it difficult to judge which produces the larger asymmetry. We thus turn to the quantitative measure of the asymmetry used in previous studies [3, 4, 7, 9]: the normalized asymmetry parameter  $\mathcal{A}(E, \varphi)$ ,

$$\mathcal{A}(E, \varphi) = \rho(E)^{-1} [\rho_{\text{up}}(E) - \rho_{\text{down}}(E)]. \quad (5)$$

For simplicity, we integrate over the whole upper and

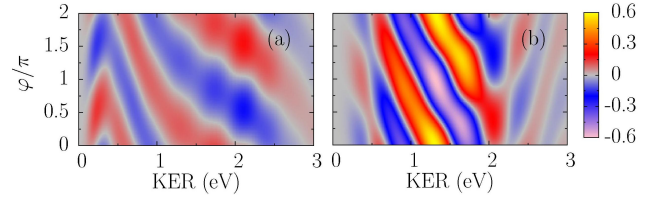


FIG. 3: (a) Asymmetry defined in Eq. (5) for the probe-only case and (b) for the pump-probe case for a  $\tau_{\text{FWHM}} = 7$  fs and  $I = 10^{14}$  W/cm $^2$  pulse.

lower hemispheres in the “up” and “down” distributions, respectively, although a narrow angular cut along the laser polarization direction might be chosen to enhance  $\mathcal{A}$  as in some experimental studies [3, 4, 9]. Figure 2 shows why such cuts are effective since the strongest CEP dependence lies at small  $\theta_K$ . Although the total energy spectrum  $\rho(E)$  in principle also depends on CEP [7], we found negligible CEP-dependence in the Franck-Condon averaged  $\rho(E)$  and thus expect essentially no contribution to the CEP dependence from the denominator of  $\mathcal{A}$ .

Figures 3(a) and 3(b) show  $\mathcal{A}(E, \varphi)$  for the probe-only and the pump-probe, respectively. For the probe-only in Fig. 3(a), we can already see reasonable asymmetry in the range 0.2–2.5 eV where it oscillates between  $-0.12$  and  $0.12$ . Comparing Fig. 3(a) and Fig. 3(b), however, we find a five-fold enhancement of  $|\mathcal{A}(E, \varphi)|$  in the pump-probe case for this intensity.

The most crucial factor determining whether an intensity-dependent effect is experimentally observable is whether it survives intensity (or focal volume) averaging. We thus intensity-averaged our results for a 7 fs laser pulse with  $\varphi = 0$  and a peak intensity of  $1.2 \times 10^{14}$  W/cm $^2$ . We used the two-dimensional geometry of Ref. [33] to perform the intensity-averaging following the procedure described in [38]. Figures 2(a), 2(e) and 3, show a clear up-down asymmetry for  $\varphi = 0$  in both probe-only and pump-probe cases, and we will check if it survives intensity averaging. Figure 4(a) shows  $\mathcal{A}(E, 0)$  before and after the intensity averaging for both cases. The corresponding total KER distributions are plotted in Fig. 4(b) to show that the small  $\rho(E)$  is the reason for the large  $\mathcal{A}(E, 0)$  at higher energies. In the pump-probe case, the intensity averaging has only been performed over the probe-pulse intensity distribution assuming that the weak pump intensity can be made uniform across the probe focal volume.

For the probe-only case, intensity averaging reduces  $\mathcal{A}$  by more than a factor of three over the entire energy range shown in Fig. 4(a) and makes it 17 times smaller for 0.5 to 1.0 eV, where  $\rho(E)$  is large and the single-intensity  $\mathcal{A}$  is largest. This significant reduction in  $\mathcal{A}$  is due to the fact that one-photon dissociation — which shows no

asymmetry — can occur for  $v \geq 7$  at very low intensities ( $\approx 10^{10}$  W/cm<sup>2</sup>). These symmetric contributions are thus amplified by the intensity averaging and swamp any asymmetry because essentially all  $v$  contribute to these KER. Figure 4(a) thus shows that intensity averaging makes it very challenging to measure CEP-effects for a single 7 fs or longer pulse in an experiment.

For the pump-probe case,  $\mathcal{A}$  is also reduced from the single intensity value — but to a much lesser extent than in the probe-only case. In fact, Fig. 4(a) shows that even after intensity averaging  $\mathcal{A}$  is an order of magnitude larger using the pump-probe scheme compared to the probe-only results. Moreover, we have found that the pump-probe scheme produces a CEP-dependent asymmetry after intensity averaging even for 10 fs pulses. These pulses are much longer than the 6 fs pulses that have been used to date to observe CEP effects [3, 10].

Besides depleting the high-lying vibrational states, the pump also impulsively aligns the molecule [43–45]). To investigate the sensitivity of  $\mathcal{A}$  to the alignment, we calculated the asymmetry for three different pump-probe time delays with aligned ( $\langle \cos^2 \theta \rangle = 0.56$ , anti-aligned ( $\langle \cos^2 \theta \rangle = 0.22$ , and dephased ( $\langle \cos^2 \theta \rangle = 0.40$  angular distributions ( $\langle \cos^2 \theta \rangle = 1/3$  for an isotropic distribution). We found that the maximum  $\mathcal{A}$  was largest for the aligned distribution, followed by the anti-aligned, with the dephased smallest. The enhancement of the aligned  $\mathcal{A}$  over the dephased was roughly 30%. For this reason we have shown here calculations for the 267 fs delay corresponding to the aligned distribution. This exercise also served to establish that the major source of the ten-fold CEP-dependent asymmetry enhancement is the depletion of the higher- $v$  states.

Another concern for experimentally observing the predicted enhancement is the fact that in our pump-probe scheme the pump pulse already produces fragments. So, separating the probe signal from the pump signal is crucial. Although the dissociating fragments from both

pulses overlap in momentum, we expect the asymmetry will still be large in a combined pump-probe signal for two reasons. First, the momentum distribution from the long pump pulse exhibits narrow peaks corresponding to higher vibrational states. Therefore, in the combined pump-probe momentum distribution, the symmetric structure would be very localized in KER, giving small overlap with the broad asymmetric signal resulting in larger asymmetry than the probe-only case. Second, we found that preparing the system actually increased the total dissociation probability of the lowest 8 vibrational states for the aligned (1.57 fold to 11.0%) and dephased (1.17 fold to 8.2%) pump-probe cases compared to the probe-only case (7.0% dissociation), thereby enhancing the ratio of the asymmetric signal to the symmetric signal.

The contrast between pump and probe signals can be further improved over the present case using pump pulses longer than 45 fs, thus increasing the depletion of the higher vibrational states and making the pump signal even more structured. A longer pulse will give more alignment, which might also enhance asymmetry. Additionally, instead of using the whole upper and lower hemispheres to define  $\mathcal{A}$ , an angular cut can be used to isolate the aligned asymmetric distribution.

As the dissociating fragments primarily lie along the laser polarization, it might be better to use orthogonal laser polarization directions for the pump and probe pulses to separate their signals [14]. For this, one might want to use the time-delay when the molecules are anti-aligned relative to the pump polarization to improve the signal. A circularly polarized pump pulse could also be used. Since depletion is the major reason for enhanced CEP effects, we believe the effect will survive using different laser polarizations. An intensity differencing scheme might also be useful to enhance asymmetry [46].

In this Letter, we have presented a prescription for substantially enhancing the CEP control of the spatial asymmetry of intense-field-induced fragmentation. We have illustrated our proposal with essentially exact, quantitative predictions for the benchmark system  $\text{H}_2^+$  and found an order of magnitude increase in the asymmetry using a relatively simple experimental technique already available in many laboratories. In addition, we have suggested several steps — besides the usual shortening of the pulse — that could increase the asymmetry even further.

We chose  $\text{H}_2^+$  for the proof of principle system due to its simplicity and our ability to treat it accurately. We expect that the principle it proves, which itself is based in part on our previously developed general picture of CEP effects, should be applicable to other more complex systems including polyatomics. That principle can be summarized as preparing the system in a single state, or narrow distribution of states, that fragment via multiple multiphoton pathways and produce the same final state of the system. Any states that fragment primarily

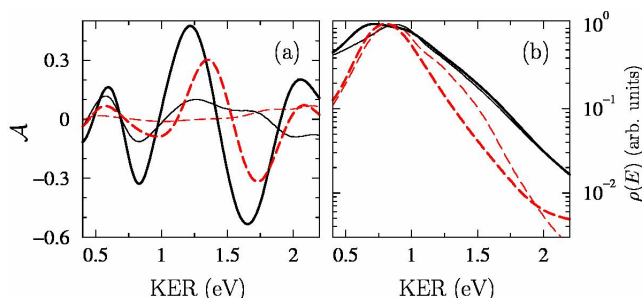


FIG. 4: (a) Asymmetry from the intensity-averaged  $\rho(E, \hat{K})$  for the probe-only (thin dashed lines) and the pump-probe (thick dashed lines) cases as well as for a single 7 fs probe pulse with a peak intensity of  $1.2 \times 10^{14}$  W/cm<sup>2</sup> (thin and thick solid lines, respectively). (b) KER distributions for the cases shown in (a) normalized to the same peak value.



with a single  $n$  will not be controllable via the CEP and should be somehow excluded from the process through, for instance, their removal.

Since the prediction of multiphoton fragmentation pathways and their final energies requires, in principle, only structural information, we believe our general picture and our proposed scheme provide a promising means for identifying CEP-controllable processes in complex molecules not readily available with other methods.

We gratefully acknowledge many useful discussions with I. Ben-Itzhak and J. McKenna regarding experimental limitations. The work was supported by the Chemical Sciences, Geo-Sciences, and Biosciences Division, Office of Basic Energy Sciences, Office of Science, U.S. Department of Energy.

- 
- [1] G. G. Paulus et al., *Nature* **414**, 182 (2001).
  - [2] V. Roudnev, B. D. Esry, and I. Ben-Itzhak, *Phys. Rev. Lett.* **93**, 163601 (2004).
  - [3] M. Kling et al., *Science* **312**, 246 (2006).
  - [4] I. Znakovskaya, P. von den Hoff, G. Marcus, S. Zhrebtsov, B. Bergues, X. Gu, Y. Deng, M. J. J. Vrakking, R. Kienberger, F. Krausz, et al., *Phys. Rev. Lett.* **108**, 063002 (2012), URL <http://link.aps.org/doi/10.1103/PhysRevLett.108.063002>.
  - [5] A. Gürtler, F. Robicheaux, W. J. van der Zande, and L. D. Noordam, *Phys. Rev. Lett.* **92**, 033002 (2004).
  - [6] V. Roudnev and B. D. Esry, *Phys. Rev. Lett.* **99**, 220406 (2007).
  - [7] J. J. Hua and B. D. Esry, *J. Phys. B* **42**, 085601 (2009).
  - [8] D. B. Milošević, G. G. Paulus, and W. Becker, *Phys. Rev. Lett.* **89**, 153001 (2002).
  - [9] M. F. Kling et al., *Mol. Phys.* **106**, 455 (2008).
  - [10] M. Kremer et al., *Phys. Rev. Lett.* **103**, 213003 (2009).
  - [11] T. Nakajima and S. Watanabe, *Phys. Rev. Lett.* **96**, 213001 (2006).
  - [12] F. Anis and B. D. Esry, *J. Phys. B* **42**, 191001 (2009).
  - [13] A. Baltuška et al., *Nature (London)* **421**, 611 (2003).
  - [14] B. Fischer et al., *Phys. Rev. Lett.* **105**, 223001 (2010).
  - [15] I. Znakovskaya, P. von den Hoff, S. Zhrebtsov, A. Wirth, O. Herrwerth, M. J. J. Vrakking, R. de Vivie-Riedle, and M. F. Kling, *Phys. Rev. Lett.* **103**, 103002 (2009).
  - [16] K. J. Betsch, D. W. Pinkham, and R. R. Jones, *Phys. Rev. Lett.* **105**, 223002 (2010).
  - [17] M. R. Thompson, M. K. Thomas, P. F. Taday, J. H. Posthumus, A. J. Langley, L. J. Frasinski, and K. Codling, *J. Phys. B* **30**, 5755 (1997), URL <http://stacks.iop.org/0953-4075/30/i=24/a=014>.
  - [18] B. Sheehy, B. Walker, and L. DiMauro, *Phys. Rev. Lett.* **74**, 4799 (1995).
  - [19] A. Bandrauk and S. Chelkowski, *Phys. Rev. Lett.* **84**, 3562 (2000).
  - [20] E. Charron, A. Giusti-Suzor, and F. H. Mies, *Phys. Rev. A* **49**, R641 (1994).
  - [21] E. Charron, A. Giusti-Suzor, and F. H. Mies, *Phys. Rev. Lett.* **71**, 692 (1993).
  - [22] E. Charron, A. Giusti-Suzor, and F. H. Mies, *Phys. Rev. Lett.* **75**, 2815 (1995).
  - [23] F. He, C. Ruiz, and A. Becker, *Phys. Rev. Lett.* **99**, 083002 (2007).
  - [24] F. He, A. Becker, and U. Thumm, *Phys. Rev. Lett.* **101**, 213002 (2008).
  - [25] D. Ray et al., *Phys. Rev. Lett.* **103**, 223201 (2009).
  - [26] K. P. Singh et al., *Phys. Rev. Lett.* **104**, 023001 (2010).
  - [27] C. R. Calvert, R. B. King, W. A. Bryan, W. R. Newell, J. F. McCann, J. B. Greenwood, and I. D. Williams, *J. Phys. B* **43**, 011001 (2010).
  - [28] The laser electric field  $\mathcal{E}_0$  in atomic units is related to the peak intensity  $I$  by  $\mathcal{E}_0 = \sqrt{I/(3.5 \times 10^{16} \text{ W/cm}^2)}$ ,  $\tau$  is related to the full width of the intensity at half maximum  $\tau_{\text{FWHM}}$  by  $\tau = \tau_{\text{FWHM}}/\sqrt{2 \ln 2}$ , and  $\omega$  is the frequency in atomic units.
  - [29] T. Wittmann et al., *Nat. Phys.* **5**, 357 (2009).
  - [30] N. G. Johnson et al., *Phys. Rev. A* **83**, 013412 (2011).
  - [31] I. Ben-Itzhak et al., *Phys. Rev. Lett.* **95**, 073002 (2005).
  - [32] F. Anis and B. D. Esry, *Phys. Rev. A* **77**, 033416 (2008).
  - [33] P. Q. Wang et al., *Phys. Rev. A* **74**, 043411 (2006).
  - [34] J. McKenna et al., *Phys. Rev. Lett.* **100**, 133001 (2008).
  - [35] J. H. Posthumus, *Rep. Prog. Phys.* **67**, 623 (2004), URL <http://stacks.iop.org/0034-4885/67/623>.
  - [36] A. Giusti-Suzor, F. H. Mies, L. F. DiMauro, E. Charron, and B. Yang, *J. Phys. B* **28**, 309 (1995), URL <http://stacks.iop.org/0953-4075/28/309>.
  - [37] J. McKenna, F. Anis, A. M. Sayler, B. Gaire, N. G. Johnson, E. Parke, K. D. Carnes, B. D. Esry, and I. Ben-Itzhak, *Phys. Rev. A* **85**, 023405 (2012), URL <http://link.aps.org/doi/10.1103/PhysRevA.85.023405>.
  - [38] V. Roudnev and B. D. Esry, *Phys. Rev. A* **76**, 023403 (2007), URL <http://link.aps.org/doi/10.1103/PhysRevA.76.023403>.
  - [39] See Fig. 2 of Ref. [38] for ionization and dissociation probabilities.
  - [40] T. A. Green and J. M. Peek, *Phys. Rev. Lett.* **21**, 1732 (1968).
  - [41] S. J. Singer, K. F. Freed, and Y. B. Band, *J. Chem. Phys.* **79**, 6060 (1983).
  - [42] F. Anis, Ph.D. thesis, Kansas State University, Manhattan, Kansas, U.S.A. (2009).
  - [43] F. Anis and B. D. Esry, *Phys. Rev. A* (2011), (to be submitted).
  - [44] I. A. Bocharova, H. Mashiko, M. Magrakvelidze, D. Ray, P. Ranitovic, C. L. Cocke, and I. V. Litvinyuk, *Phys. Rev. A* **77**, 053407 (2008).
  - [45] H. Stapelfeldt and T. Seideman, *Rev. Mod. Phys.* **75**, 543 (2003).
  - [46] P. Q. Wang et al., *Opt. Lett.* **30**, 664 (2005).